International Journal of Environmental Science and Technology (2019) 16:7221–7228
https://doi.org/10.1007/s13762-019-02401-8

ORIGINAL PAPER

Mechanisms of mercury removal from aqueous solution by high-fixation hydroxyapatite sorbents

N. S. de Resende[1] · C. L. M. Camargo[2] · P. C. Reis[3] · C. A. C. Perez[4] · V. M. M. Salim[1]

Received: 28 February 2019 / Revised: 4 May 2019 / Accepted: 8 May 2019 / Published online: 13 May 2019

Abstract

Hydroxyapatite is an effective adsorbent for mercury removal from aqueous solutions, although capture mechanisms are not yet clearly understood. The purpose here is to investigate the type of interactions between mercury and the surface sites as well as intraparticle diffusion mechanism in this sorbent, correlating with the mercury immobilization by hydroxyapatite. Physicochemical properties of a synthetic nano-hydroxyapatite were determined by nitrogen adsorption isotherms at 77 K, X-ray fluorescence, field emission gun scanning electron microscopy, and X-ray powder diffraction techniques. Both fresh and spent sorbent samples were analyzed using X-ray powder diffraction to assess the structural changes on hydroxyapatite crystalline lattice during the mercury sorption process. Rietveld refinement of powder X-ray diffraction data allowed insights into the mechanisms of Hg^{2+} sorption on synthetic hydroxyapatite. Kinetics and Rietveld refinement results revealed the immobilization of mercury in the spent sorbent, suggesting that this process takes place at two steps: (1) the mercury complexation with surface phosphate sites of hydroxyapatite followed by (2) the slower mercury diffusion along with its incorporation inside the hydroxyapatite crystalline lattice. Furthermore, the results on thermal stability confirmed the mercury immobilization by hydroxyapatite, characterizing the spent sorbent as a non-hazardous material and minimizing the environmental impacts of solid waste disposal.

Keywords Hydroxyapatite · Mercury immobilization · Non-hazardous spent sorbent · Removal mechanisms · Rietveld refinement

Introduction

As one of the most toxic heavy metals in the environment, mercury (Hg) has its adverse effects on the ecosystem and human health aggravated due to its bioaccumulative properties (Driscoll et al. 2013; Henriques et al. 2015; Obrist et al. 2018). Indeed, mercury as a global pollutant has been widely discussed by the international government agencies and the scientific community, demanding efforts to reduce its emissions by the development of new emission control technologies (UNEP 2013; Lin et al. 2017; Chen et al. 2018).

Conventional methods for removing inorganic mercury from industrial wastewaters include sulfide precipitation (Jeong et al. 2007), coagulation (Henneberry et al. 2011), ion exchange (Asasian and Kaghazchi 2013), and adsorption (Zhang et al. 2014; Xu et al. 2016; Deliz Quiñones et al. 2016; Naushad et al. 2016; Attari et al. 2017). Hydroxyapatite (HAp) has been pointed out as a promising material for heavy metal removal, especially mercury, from wastewater (Oliva et al. 2011; Kim and Lee 2014). Hexagonal HAp—$Ca_{10}(PO_4)_6(OH)_2$—is a crystalline structure consisting of columns of calcium and oxygen parallel to the hexagonal axis. HAp has two non-equivalent Ca sites: the site I which contains Ca^{2+} ions in a columnar arrangement, coordinated to nine oxygen atoms of PO_4^{3-} groups, and

Editorial responsibility: Fatih ŞEN.

✉ N. S. de Resende
neuman@peq.coppe.ufrj.br

[1] Programa de Engenharia Química, PEQ-COPPE, Centro de Tecnologia, Universidade Federal do Rio de Janeiro–UFRJ, Bl. G/115 – Cidade Universitária, Rio de Janeiro, RJ 21941-914, Brazil

[2] Escola de Química, Universidade Federal do Rio de Janeiro–UFRJ, Rio de Janeiro, RJ, Brazil

[3] Instituto Nacional de Proteção Industrial– INPI, Rio de Janeiro, RJ, Brazil

[4] Instituto Federal de Ciência e Tecnologia do Rio de Janeiro - IFRJ, Rio de Janeiro, RJ, Brazil

the site II where Ca^{2+} is hepta-coordinated to six oxygen atoms of five PO_4^{3-} groups and one OH^- group (El Feki et al. 1999). Different cations can substitute Ca^{2+} ions in the HAp lattice. Large divalent cations replace Ca^{2+} at Ca II sites, whereas small divalent ones replace Ca^{2+} at Ca I sites (Guerra-López et al. 2001). The charge compensation mechanism has a substantial influence on the apatite structure; thereby, Rietveld refinement of X-ray powder diffraction data has been used to investigate these substitution mechanisms (Young 1993; El Feki et al. 1999; Wilson et al. 2003; Lala et al. 2016).

As a result of its amphoteric character, the surface chemical properties of HAp (strength of the acid and base sites) may be changed, depending on the pH value of the solution (Resende et al. 2006). Besides, the interactions between mercury and HAp can occur at a bulk level with the mercury incorporation into the HAp crystalline matrix. In short, mechanisms of mercury removal by HAp include complexation (Kim and Lee 2014), dissolution of HAp and precipitation of metal phosphates (Oliva et al. 2011), Hg(II) diffusion into apatite structure (Jeanjean et al. 1996), ion exchange with calcium ions (Corami et al. 2008), or a combination of some of these (Ferri et al. 2019). However, there are still significant uncertainties regarding the occurrence of such mechanisms.

This paper presents the investigation on the sorption mechanisms of mercury (Hg(II)) removal from aqueous solution using a synthetic nano-HAp sorbent. This study is a part of a long-term research project about mercury removal from liquid and gaseous streams carried out during the last decade at Hg-laboratory at Chemical Engineering Program (PEQ–UFRJ). It is noteworthy that this project aims at the global decontamination of mercury, developing high-efficiency materials for the mercury capture as well as its immobilization in a single process.

Kinetic studies were carried out in batch adsorption systems using synthesized HAp, which were characterized by nitrogen adsorption isotherms at 77 K, X-ray fluorescence (XRF), field emission gun scanning electron microscopy (FEG-SEM), and X-ray diffraction (XRD) techniques. Rietveld refinement of XRD results allowed the evaluation of structural modifications on HAp crystal lattice during the mercury sorption process. In addition, the thermal stability of mercury in the spent Hg-HAp sorbent was evaluated and correlated with removal mechanisms.

Materials and methods

Sorbent synthesis

HAp was prepared by slowly adding a 0.3 M diammonium hydrogen phosphate—$(NH_4)_2{\cdot}HPO_4$ (Merck)—aqueous solution to a 0.5 M calcium nitrate tetrahydrate—$Ca(NO_3)_2{\cdot}4H_2O$ (Merck)—aqueous solution at 353 K and pH = 10. Concentrated NH4OH (Merck) was used to maintain the pH of the solution. The precipitate was washed and filtrated several times with ultrapure water at 353 K until the elimination of residual alkalis. The drying of the final solid was at 353 K for 24 h. A more detailed description of HAp preparation was given elsewhere (Resende et al. 2006; Camargo et al. 2018).

Physicochemical characterization

The chemical composition of HAp was determined by XRF spectrometer (RIX-3100, Rigaku) with rhodium tube as X-ray source. Nitrogen physisorption isotherms obtained at 77 K on Micromeritics® ASAP 2000 instrument were used to determine textural properties. Specific surface area (S_{BET}) and average pore diameter were calculated employing BET (Brunauer, Emmett, and Teller) and BJH (Barrett, Joyner, and Halenda) methods, respectively. The morphology of the sorbent was examined by field emission gun scanning electron microscope (FEG-SEM Quanta 400, FEI Company). XRD patterns were obtained on a Miniflex-Rigaku powder diffractometer with Cu-Kα radiation ($\lambda = 1.5418$ Å) by scanning from 10° to 100° (2θ).

Sorption tests

Batch sorption experiments were carried out in 100-mL polycarbonate bottles containing 0.2 g of HAp. Each bottle received a constant volume (50 mL) of $HgCl_2$ (Merck) solution with mercury concentrations of 100 and 200 mg L^{-1}. After closing, the systems were shaken at 200 rpm (Shaker model G24, New Brunswick Scientific) at 298 K for the specified time (from 2 to 360 h), with pH monitoring during the first 4 h. Then, the suspensions were centrifuged at 1500 rpm for 15 min. Mercury concentrations in the supernatant were determined by atomic absorption spectrophotometry (AAS) using a PerkinElmer 1100 B spectrophotometer. Due to the low detection limit of this technique, about 0.5 ppm Hg(II) (Chilov 1975), a preconcentration step is not required for mercury assay.

Crystal structure evaluation

The crystal structures of the fresh and spent HAp sorbent (before and after adsorption, respectively) were refined by Rietveld method (FULLPROF suite software) using the HAp structure by Hughes et al. (1989) as a starting point. The main refined parameters were the scale factor, unit cell parameters, occupancy factors of calcium (Ca)–phosphorus (P), background polynomial coefficients, and peak shapes. Modifications on the sorbent crystal structure during

the adsorption process were evaluated by monitoring the changes in the crystal lattice parameters.

Thermal stability tests

The mobile mercury species on the spent sorbent were removed by heating the sample from 298 K up to 423 K for 1 h in a vacuum oven. The immobilized mercury amount in the HAp sorbents was determined by comparing XRF results, before and after the heat treatment.

Results and discussion

Physicochemical properties

Textural characterization results showed a mesoporous sorbent with an average pore diameter of 146 Å and a high BET surface area of 49 m^2g^{-1}. The SEM micrograph of HAp is given in Fig. 1, and it can be seen that HAp sorbent exhibits rod-like nanocrystalline particles. The Ca/P molar ratio of 1.57 determined in XRF results characterized the sorbent as calcium (Ca)-deficient HAp with the chemical formula of $Ca_{9.42}(HPO_4)_{0.58}(PO_4)_{5.42}(OH)_{1.42}$. The protonation of the nearest $(PO_4)^{3-}$ ion maintains the charge balance for each Ca vacancy, with the formation of $(HPO_4)^{2-}$ and loss of nearest $(OH)^-$ (Wilson et al. 2003). XRD pattern of HAp is shown in "Rietveld refinement results" section along with the analogous results for the spent sorbent.

Sorption kinetic results

The kinetic results for Hg(II) initial concentrations of 100 mg L^{-1} (Fig. 2a) point out the fast mercury uptake during the first 30 min, in the pH range from 3.5 to 5. In this range, ≡POH groups dominate over other surface groups; likewise, Hg(II) prevails over hydrolyzed mercury species

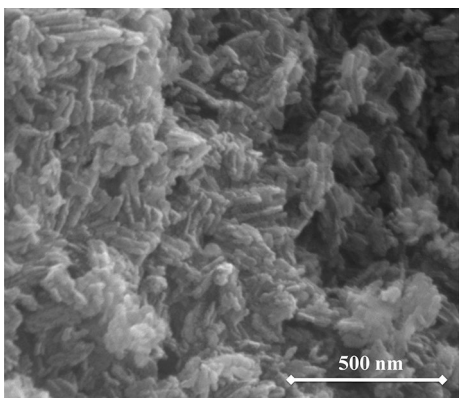

Fig. 1 SEM image of the synthetic HAp at a magnification of 100 kx

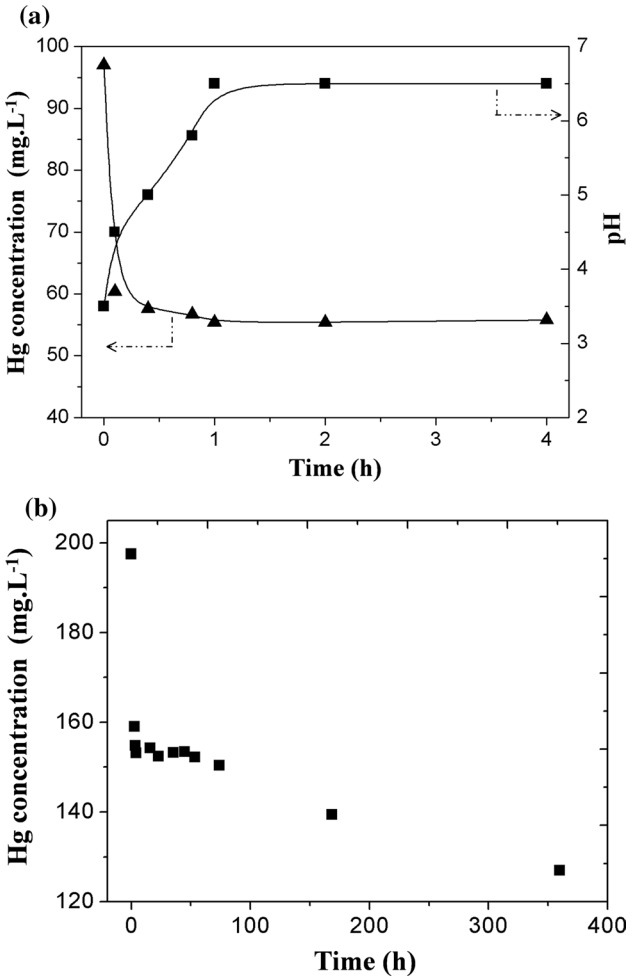

Fig. 2 Kinetics of Hg(II) sorption on the HAp sorbent. Systems with Hg(II) initial concentration of: **a** 100 mg L^{-1} (with pH monitoring) and **b** 200 mg L^{-1}

(Powell et al. 2005). After the first 30 min, pH increased up to 6.5—the point of zero charge (PZC) of HAp and mercury concentration reached a constant value. At pH near PZC the dominant groups are ≡PO^- and ≡$CaOH_2^+$ (Wu et al. 1991; Corami et al. 2008). The significant reduction in mercury uptake rate at pH around PZC indicated that ≡POH group was responsible for the fast mercury uptake surface complexation at the beginning of the sorption process. Although mercury complexation on the HAp surface has partially displaced H^+ ions, it was the large HAp buffering capacity (Smičiklas et al. 2000) that explained the increase in the pH value shown in Fig. 2a.

A second sorption test was performed for 400 h (Fig. 2b) to verify if the sorption equilibrium was reached even for long contact time using a Hg(II) initial concentration of 200 mg L^{-1}. At the beginning of the sorption process, a fast uptake of Hg(II) was observed, as well as in the previous case (Hg(II) initial concentration of 100 mg L^{-1}). However,

the negative slope on mercury concentration vs time graph, even after 50 h of contact time, indicates the occurrence of another phenomenon in addition to the fast Hg(II) surface complexation.

The literature suggests many possible heavy metal removal mechanisms by HAp such as surface adsorption (Kim and Lee 2014), dissolution/precipitation of phosphate metal (Oliva et al. 2011), metal diffusion into apatite structure (Jeanjean et al. 1996), ion exchange, and ion metal occupancy of Ca vacancies (Corami et al. 2008), or a combination of these mechanisms. Here, Rietveld refinement was applied as a helpful tool to provide some insights into these mechanisms.

Rietveld refinement results

The XRD patterns (Fig. 3), collected at different contact times to evaluate the structural modifications of the HAp during Hg(II) sorption tests, were refined according to the Rietveld method. XRD results revealed characteristic peaks of pure crystalline and hexagonal HAp for both fresh and spent sorbent samples. No additional peaks in the spent sorbent XRD pattern indicate any additional crystalline phases produced during sorption tests. However, the Rietveld refinement results (Table 1), for both fresh and spent sorbents, reveal that Hg(II) sorption causes significant changes in unit cell parameters of the crystalline structure, mainly in the *a* parameter (reduction of 0.0015 Å, $\sigma = 0.0002$). Crystallite size remains nearly constant throughout the sorption test.

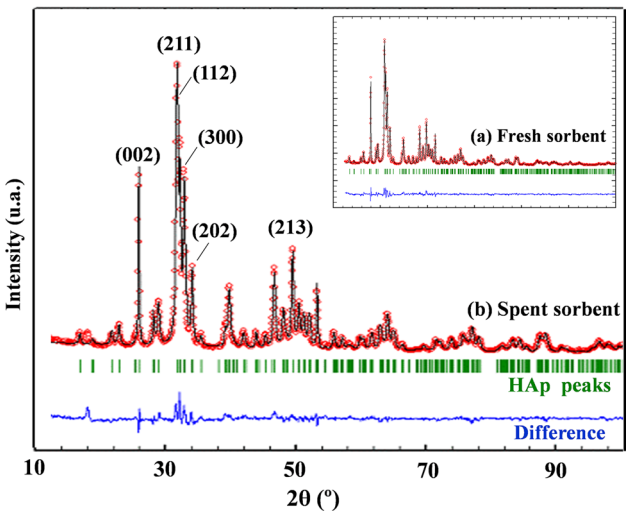

Fig. 3 Experimental XRD results for the fresh sorbent (**a**) and the spent sorbent (**b**). Vertical lines mark the positions of the Bragg peaks for the HAp. The red circles are the calculated intensities by Rietveld refinement, and the blue lines are differences between experimental and calculated intensities

Table 1 also presents refined occupancy factors. Vacancies on Ca II sites revealed a non-stoichiometric HAp structure at the beginning of the test (contact time of zero hours). The rise in the calcium occupancy during the sorption test, especially on Ca II sites, indicates the mercury incorporation on these vacancies. These results are in agreement with the findings from other studies: Small divalent cations replace Ca^{2+} at Ca I sites, whereas large divalent ones as Hg(II) replace Ca^{2+} at Ca II sites (Guerra-López et al. 2001). Besides, the reduction in refined unit cell parameters endorses the mercury incorporation on Ca II sites, once Hg(II) has a slightly smaller ionic radius than Ca^{2+} ions. An increase in the OH-occupancy, which is required to maintain the electroneutrality of the system after the mercury entrance, also confirmed this mechanism. Thus, the Rietveld refinement results confirmed a slow mechanism of mercury incorporation into the crystalline matrix of HAp in addition to the rapid surface complexation phenomenon at the beginning of the process (Fig. 4a). As illustrated in Fig. 4b, the Hg(II) ion occupied the vacant Ca(II) site inside the HAp crystal lattice. Once the Hg(II) ions become part of the HAp crystal lattice, the slow mechanism of mercury incorporation is responsible for the high performance for the increased mercury capacity as well as the mercury immobilization in HAp sorbents.

Thermal stability results

Finally, thermal stability results (Fig. 5) confirm that a portion of captured Hg(II) was released during the heating, while another part remained fixed on the spent sorbent. The

Table 1 Rietveld refinement results for fresh sorbent and used sorbent (after 48, 72, and 150 h of contact time during Hg(II) sorption tests)

Contact time (h)	Unit cell parameters (Å) ($\sigma = 0.0002$)		Crystal size (Å)		Occupancy factors			
	a	*c*	hk0	00l	Ca I ($\sigma = 0.04$)	Ca II ($\sigma = 0.05$)	P ($\sigma = 0.05$)	OH ($\sigma = 0.01$)
0	9.4367	6.8774	216	513	4.00	5.66	5.84	1.57
48	9.4351	6.8766	215	548	4.11	6.07	5.99	2.10
72	9.4349	6.8772	214	568	4.06	6.98	5.96	1.95
150	9.4352	6.8767	215	548	3.99	5.92	5.89	1.92

*σ standard deviation

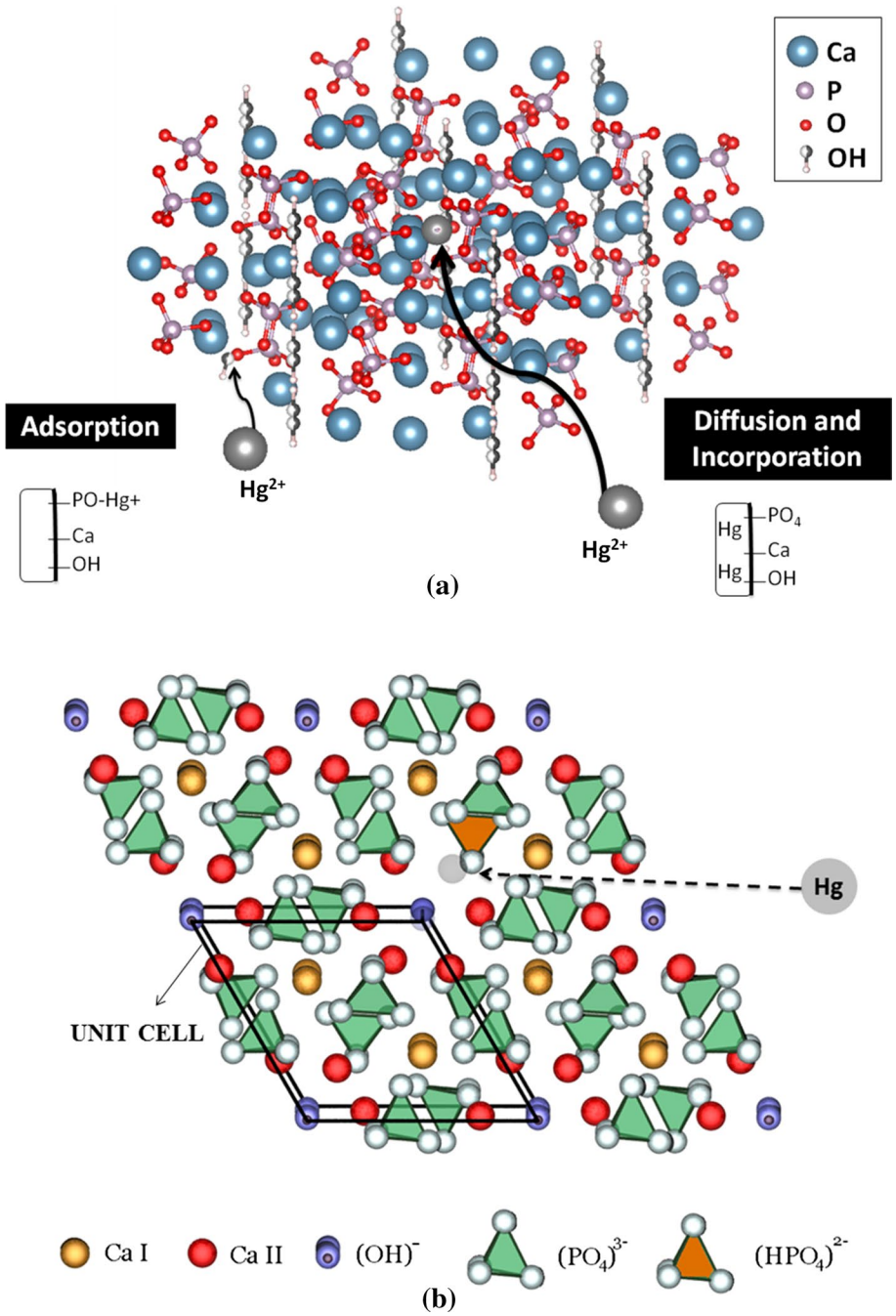

Fig. 4 **a** 3D representation of the sorption mechanisms on HAp; **b** representation of HAp crystal lattice with Hg(II) occupying the vacancies on Ca II sites

increase in the amount of fixed mercury as a function of the contact time indicates some transfer mass limitation of Hg(II) diffusion process into the solid matrix and the occupation of Ca vacancies.

These results corroborated the proposed removal mechanisms: Released mercury at low temperature is supposed to be related to the Hg(II) captured by surface complexation mechanism (weak interaction with phosphate sites: Hg « ≡POH), whereas immobilized mercury is related to stronger interaction forces of the mercury incorporation into the HAp crystal lattice. Therefore, besides the high mercury removal capacity, the second mechanism endorses that synthetic hydroxyapatite-based sorbents are able to also immobilize mercury in its structure.

The uptake of other metal ions by HAp was also observed to be similar. For instance, intracrystalline diffusion with the incorporation of cadmium into HAp structure enables in situ immobilization of cadmium followed by its storage in a single process (Marchat et al. 2007). While traditional adsorbents typically require additional treatments before final disposal (Piao and Bishop 2006; Zhang et al. 2009; Fu and Wang 2011; Carolin et al. 2017), hydroxyapatite

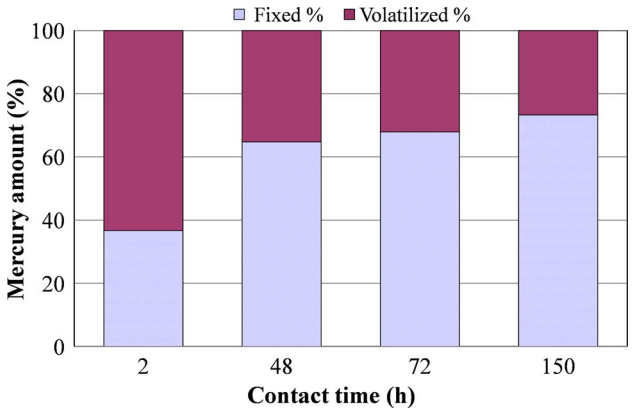

Fig. 5 Effect of contact time on mercury immobilization by the HAp sorbent

promotes both mercury decontamination and storage in the same material, avoiding the need for further purification procedure steps such as the stabilization process of the spent sorbent.

Conclusion

The non-stoichiometric nano-HAp synthesized with 49 $m^2\ g^{-1}$ was proved to be an efficient sorbent for mercury removal and immobilization. Kinetic results of Hg(II) sorption indicated that mercury interacts with the HAp sorbent in two different ways. The proposed mechanism includes a surface complexation through weak interactions between Hg(II) and POH sites (Hg « ≡POH) and slower diffusion of Hg(II) ions into HAp solid matrix with the occupation of calcium vacancies.

Rietveld refinement method was a useful and reliable tool to elucidate the removal mechanisms through the assessment of sorbent crystallographic parameters during the sorption tests. Results of (a) reduction in unit cell parameters and (b) increase in both calcium and (OH^-) occupancy endorsed the mercury immobilization mechanism on HAp lattice by the occupation of vacancies or replacement of Ca^{2+} ions. Finally, thermal stability results revealed that the mercury fixation increased with the contact time, corroborating the mercury migration mechanism into the HAp crystalline lattice.

Based on these results, hydroxyapatite was proved to be a promising sorbent for Hg(II) removal once the mercury incorporation inside the crystalline matrix promotes its immobilization. Hence, the spent Hg-HAp sorbent could be considered as a non-hazardous material for disposal purposes reducing the risks associated with the solid waste disposal. Future works include the investigation of other possible mechanisms, aiming at the development of an adsorbent with performance adjusted for the global mercury decontamination.

Acknowledgements The authors gratefully acknowledge the financial support by the following Brazilian agencies: CNPq—National Council of Scientific and Technological Development and FAPERJ—Fundação de Amparo à Pesquisa do Estado do Rio de Janeiro.

References

Asasian N, Kaghazchi T (2013) A comparison on efficiency of virgin and sulfurized agro-based adsorbents for mercury removal from aqueous systems. Adsorption 19:189–200. https://doi.org/10.1007/s10450-012-9437-8

Attari M, Bukhari SS, Kazemian H, Rohani S (2017) A low-cost adsorbent from coal fly ash for mercury removal from industrial wastewater. J Environ Chem Eng 5:391–399. https://doi.org/10.1016/J.JECE.2016.12.014

Camargo CLM, Salim VMM, Tavares FW, de Resende NS (2018) Phenomenological modeling for elemental mercury capture on hydroxyapatite-based adsorbents: an experimental validation. Fuel 225:509–518. https://doi.org/10.1016/j.fuel.2018.03.177

Carolin CF, Kumar PS, Saravanan A et al (2017) Efficient techniques for the removal of toxic heavy metals from aquatic environment: a review. J Environ Chem Eng 5:2782–2799. https://doi.org/10.1016/J.JECE.2017.05.029

Chen CY, Driscoll CT, Eagles-smith CA et al (2018) A critical time for mercury science to inform global policy. Environ Sci Technol. https://doi.org/10.1021/acs.est.8b02286

Chilov S (1975) Determination of small amounts of mercury. Talanta 22:205–232. https://doi.org/10.1016/0039-9140(75)80059-2

Corami A, Mignardi S, Ferrini V (2008) Cadmium removal from single- and multi-metal () solutions by sorption on hydroxyapatite. J Colloid Interface Sci 317:402–408. https://doi.org/10.1016/j.jcis.2007.09.075

Deliz Quiñones K, Hovsepyan A, Oppong-Anane A, Bonzongo J-CJ (2016) Insights into the mechanisms of mercury sorption onto aluminum based drinking water treatment residuals. J Hazard Mater 307:184–192. https://doi.org/10.1016/j.jhazmat.2016.01.001

Driscoll CT, Mason RP, Chan HM et al (2013) Mercury as a global pollutant: sources, pathways, and effects. Environ Sci Technol 47:4967–4983. https://doi.org/10.1021/es305071v

El Feki H, Savariault JM, Ben Salah A (1999) Structure refinements by the Rietveld method of partially substituted hydroxyapatite: ca9Na0.5(PO4)4.5(CO3)1.5(OH)2. J Alloys Compd 287:114–120. https://doi.org/10.1016/S0925-8388(99)00070-5

Ferri M, Campisi S, Scavini M et al (2019) In-depth study of the mechanism of heavy metal trapping on the surface of hydroxyapatite. Appl Surf Sci 475:397–409. https://doi.org/10.1016/J.APSUSC.2018.12.264

Fu F, Wang Q (2011) Removal of heavy metal ions from wastewaters: a review. J Environ Manage 92:407–418. https://doi.org/10.1016/j.jenvman.2010.11.011

Guerra-López J, Pomés R, Della Védova CO et al (2001) Influence of nickel on hydroxyapatite crystallization. J Raman Spectrosc 32:255–261. https://doi.org/10.1002/jrs.689

Henneberry YK, Kraus TEC, Fleck JA et al (2011) Removal of inorganic mercury and methylmercury from surface waters following coagulation of dissolved organic matter with metal-based salts. Sci Total Environ 409:631–637. https://doi.org/10.1016/j.scitotenv.2010.10.030

Henriques B, Rocha LS, Lopes CB et al (2015) Study on bioaccumulation and biosorption of mercury by living marine macroalgae: prospecting for a new remediation biotechnology applied to saline waters. Chem Eng J 281:759–770. https://doi.org/10.1016/J.CEJ.2015.07.013

Hughes JM, Cameron M, Crowley KD (1989) Structural variations in natural F, OH, and Cl apatites. Am Mineral 74:870–876

Jeanjean J, Mcgrellis S, Rouchaud JC et al (1996) A crystallographic study of the sorption of cadmium on calcium hydroxyapatites: incidence of cationic vacancies. J Solid State Chem 126:195–201

Jeong HY, Klaue B, Blum JD, Hayes KF (2007) Sorption of mercuric ion by synthetic nanocrystalline mackinawite (FeS). Environ Sci Technol. https://doi.org/10.1021/ES070289L

Kim Y, Lee YJ (2014) Characterization of mercury sorption on hydroxylapatite: batch studies and microscopic evidence for adsorption. J Colloid Interface Sci 430:193–199. https://doi.org/10.1016/j.jcis.2014.05.028

Lala S, Ghosh M, Das PK et al (2016) Magnesium substitution in carbonated hydroxyapatite: structural and microstructural characterization by Rietveld's refinement. Mater Chem Phys 170:319–329. https://doi.org/10.1016/J.MATCHEMPHYS.2015.12.058

Lin Y, Wang S, Steindal EH et al (2017) A holistic perspective is needed to ensure success of minamata convention on mercury. Environ Sci Technol 51:1070–1071. https://doi.org/10.1021/acs.est.6b06309

Marchat D, Bernache-Assollant D, Champion E (2007) Cadmium fixation by synthetic hydroxyapatite in aqueous solution—thermal behaviour. J Hazard Mater 139:453–460. https://doi.org/10.1016/J.JHAZMAT.2006.02.040

Naushad M, Ahamad T, Sharma G et al (2016) Synthesis and characterization of a new starch/SnO2 nanocomposite for efficient adsorption of toxic Hg2+ metal ion. Chem Eng J 300:306–316. https://doi.org/10.1016/J.CEJ.2016.04.084

Obrist D, Kirk JL, Zhang L et al (2018) A review of global environmental mercury processes in response to human and natural perturbations: changes of emissions, climate, and land use. Ambio 47:116–140. https://doi.org/10.1007/s13280-017-1004-9

Oliva J, De Pablo J, Cortina J-L et al (2011) Removal of cadmium, copper, nickel, cobalt and mercury from water by Apatite II™: column experiments. J Hazard Mater 194:312–323. https://doi.org/10.1016/J.JHAZMAT.2011.07.104

Piao H, Bishop PL (2006) Stabilization of mercury-containing wastes using sulfide. Environ Pollut 139:498–506. https://doi.org/10.1016/j.envpol.2005.06.005

Powell KJ, Brown PL, Byrne RH et al (2005) Chemical speciation of environmentally significant heavy metals with inorganic ligands. Part 1: the $Hg2^{+}$–Cl–, OH–, CO32–, SO42–, and PO43– aqueous systems (IUPAC Technical Report). Pure Appl Chem 77:739–800. https://doi.org/10.1351/pac200577040739

Resende NS, Nele M, Salim VMM (2006) Effects of anion substitution on the acid properties of hydroxyapatite. Thermochim Acta 451:16–21. https://doi.org/10.1016/j.tca.2006.08.012

Smičiklas I, Milonjić S, Pfendt P, Raičević S (2000) The point of zero charge and sorption of cadmium (II) and strontium (II) ions on synthetic hydroxyapatite. Sep Purif Technol 18:185–194. https://doi.org/10.1016/S1383-5866(99)00066-0

United Nations Environment Programme (UNEP) (2013) Global mercury assessment. sources, emissions, releases and environmental transport. UNEP-Chemicals, Geneva, Switzerland. https://wedocs.unep.org/bitstream/handle/20.500.11822/11401/GlobalMercuryAssessment2013.pdf?sequence=1&isAllowed=y

Wilson RM, Elliott JC, Dowker SEP (2003) Formate incorporation in the structure of Ca-deficient apatite: Rietveld structure refinement. J Solid State Chem 174:132–140. https://doi.org/10.1016/S0022-4596(03)00188-9

Wu L, Forsling W, Schindler PW (1991) Surface complexation of calcium minerals in aqueous solution: 1. Surface protonation at fluorapatite—water interfaces. J Colloid Interface Sci 147:178–185. https://doi.org/10.1016/0021-9797(91)90145-X

Xu X, Schierz A, Xu N, Cao X (2016) Comparison of the characteristics and mechanisms of Hg(II) sorption by biochars and activated carbon. J Colloid Interface Sci 463:55–60. https://doi.org/10.1016/J.JCIS.2015.10.003

Young RA (1993) The Rietveld method. International Union of Crystallograhy, Cambridge

Zhang X-Y, Wang Q-C, Zhang S-Q et al (2009) Stabilization/solidification (S/S) of mercury-contaminated hazardous wastes using thiol-functionalized zeolite and Portland cement. J Hazard Mater 168:1575–1580. https://doi.org/10.1016/J.JHAZMAT.2009.03.050

Zhang X, Jia X, Zhang G et al (2014) Efficient removal and highly selective adsorption of Hg2+ by polydopamine nanospheres with total recycle capacity. Appl Surf Sci 314:166–173. https://doi.org/10.1016/J.APSUSC.2014.06.158